Neural Network Ensemble for Precise Laser Spot Position Determination on a Quadrant Detector

Micah Baleya, Hossam Shalaby, *Senior Member, IEEE*, Kazutoshi Kato, *Senior Member, IEEE*, and Maha Elsabrouty, *Senior Member, IEEE*

Abstract— A quadrant detector (QD) is a widely used technology for laser spot position sensing in establishing and maintaining laser communication links. There is a nonlinear relationship between the output signal offset and the precise location of the laser spot on the QD, which impairs position detection accuracy. To address the problem, this work employs a neural network ensemble solution. An ensemble of neural networks combines the predictive power of multiple artificial neural network (ANN) models, resulting in improved generalization and prediction stability compared to a single neural network. Test results indicate that our solution demonstrates a significant improvement in both the estimated position error and the generalization capability when compared to individual ANN solutions.

Index Terms— Quadrant detector, radial basis neural network, feedforward neural network, artificial neural network, neural network ensemble, laser communication.

I. Introduction

RECENTLY, a plethora of research focusing on laser communications has emerged in an attempt to complement RF based communication systems, which for years, prevailed the communication scene [1]. Laser technology uses smaller sized components that are lighter and require less power consumption to achieve higher data transmission rates compared to the RF counterpart, while employing narrow and directional beams of light [2], [3]. The quadrant detector (QD) senses the incident light spot and generates photoelectric signals reflecting the position of the light spot on its surface, with fast response and high resolution, enabling position detection and tracking [4]. Nevertheless, the relationship between spot position on QD and the output signal offset (OSO) is nonlinear. This results in high detection accuracy of light spot position around QD center. However, as the spot moves further away

from the center, the measurements become less accurate. It should be noted that the accuracy of QD detection affects the accuracy and stability of the subsequent modules in the receiver.

In mitigating QD detection non-linearities, several solutions have emerged in the literature. These solutions range between classical techniques, e.g., curve fitting [5], [6], [7], and ANN-based methods. ANN have proven to be superior in performance and provide better fit for modelling non-linearities.

In [8], an optimized Feedforward Neural Network (FFNN) model is developed using backpropagation learning and the Levenberg-Marquardt (LM) algorithm. The developed model achieved superior performance compared to the fusion method and eight-order polynomial fitting. To tackle the challenge of collecting sufficient data from the actual QD for training an ANN, reference [9] generates QD simulation data using mathematical formulas. A small amount of actual data and the simulation data constitute the dataset for training a FFNN model. The proposed solution outperforms the approach in [8] as well as the geometric approximation method described in [10]. In [11], a method for detecting x and y coordinates for the light spot position using Radial Basis Function Neural Network (RBFNN) model is proposed. The developed model outperformed both the FFNN in [8] and seventh-order polynomial fitting.

However, all these studies used a single ANN solution. Individually, ANN models have their own intrinsic limitations. An ANN cannot provide a definitive solution for generalizing a problem [12], as it cannot fully learn all the complex underlying features, leading to poor generalization in some parts of the dataset. In this letter, an innovative solution of neural network ensemble is proposed. Ensemble learning enhances the stability of spot position predictions and improves accuracy, by providing better generalization beyond the learned dataset. Further, this solution can easily be extended to any position detection system where higher prediction accuracy beyond that of a single ANN is sought after.

II. Laser Spot Position Determination on Quadrant Detector

The QD is a photosensitive surfaced sensor that is used in position determination, alignment, and tracking systems. It is made up of four symmetrical P-N junction photodiodes
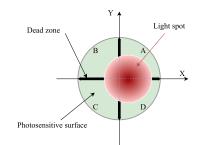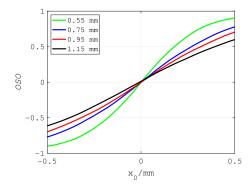
Fig. 1.   QD and incident light spot.

Fig. 2.   Output Signal Offset(OSO) vs. **x**-axis beam displacement on the QD with varied beam radii.

(Quadrants), which are isolated by a narrow dead zone as depicted in Fig. 1.

Light falling on the surface of the detector triggers each photodiode to generate photoelectric signals. The position of incident light in relation to the detector's center is estimated at every instance of time by combining the magnitudes of electrical signals from the four photodiodes to obtain the OSO [13]. The OSO formula assumes that the spot touches all the quadrants, as illustrated in Fig. 1 and the OSO is calculated as follows:

$$\hat{x} = \frac{(I_A + I_D) - (I_B + I_C)}{I_A + I_B + I_C + I_D},$$
$$\hat{y} = \frac{(I_A + I_B) - (I_C + I_D)}{I_A + I_B + I_C + I_D}, \qquad (1)$$

where $\hat{x}$ and $\hat{y}$ represent the degree to which the beam has deviated from QD origin in the x and y directions. I_A, I_B, I_C, and I_D are the photoelectric signals from the quadrants.

Using (1), provides a good estimation around the QD center. However, laser spot's movement across the QD is not accurately reflected in the OSO. Figure 2 illustrates the OSO derived from experimental data from QD, considering various beam radii. Also, the figure shows the relationship between the expected spot position and the size of beam radius.

The light spot energy $h(x, y)$ can be approximated by a Gaussian distribution as follows [5]:

$$h(x, y) = \frac{2P_0}{\pi \omega^2} \exp\left(-\frac{2\left((x - x_0)^2 + (y - y_0)^2\right)}{\omega^2}\right), \qquad (2)$$

where (x_0, y_0) is the coordinate for the light spot center, P_0 represents the aggregate spot energy, while ω denotes the

beam's radius. The photoelectric current from each quadrant is obtained by integrating the energy intercepted over the area that the spot covers in each individual photodiode, as follows:

$$I_i \propto \iint\limits_{S_i} h(x, y)\, dx\, dy\ (i = A, B, C, D), \qquad (3)$$

where S_i is the area covered by spot in each photodiode. In getting the true spot position value the following is used,

$$\hat{x} = \frac{\iint\limits_{S_A + S_D} h(x, y)\, dx\, dy - \iint\limits_{S_B + S_C} h(x, y)\, dx\, dy}{\iint\limits_{S_A + S_D} h(x, y)\, dx\, dy + \iint\limits_{S_B + S_C} h(x, y)\, dx\, dy},$$

$$\hat{y} = \frac{\iint\limits_{S_A + S_B} h(x, y)\, dx\, dy - \iint\limits_{S_C + S_D} h(x, y)\, dx\, dy}{\iint\limits_{S_A + S_B} h(x, y)\, dx\, dy + \iint\limits_{S_C + S_D} h(x, y)\, dx\, dy}. \qquad (4)$$

A simplified expression is obtained by employing infinite integral method, resulting in the errors of the Gaussian spot in the position of x and y as follows:

$$\hat{x} = \frac{4}{\pi \omega^2} \left(\int\limits_{-\infty}^{\infty} \frac{2(y - x_0)^2}{\omega^2}\, dy \int\limits_{0}^{\infty} \frac{-2(x - y_0)^2}{\omega^2}\, dx\right)$$
$$= \mathrm{erf}\left(\frac{\sqrt{2}x_0}{\omega}\right),$$

$$\hat{y} = \frac{4}{\pi \omega^2} \left(\int\limits_{-\infty}^{\infty} \frac{2(y - x_0)^2}{\omega^2}\, dy \int\limits_{0}^{\infty} \frac{-2(x - y_0)^2}{\omega^2}\, dx\right)$$
$$= \mathrm{erf}\left(\frac{\sqrt{2}y_0}{\omega}\right), \qquad (5)$$

where erf(.) is error function. The approximate spot position can then be obtained as follows:

$$x_0 = \omega \frac{\mathrm{erf}^{-1}(\hat{x})}{\sqrt{2}},$$
$$y_0 = \omega \frac{\mathrm{erf}^{-1}(\hat{y})}{\sqrt{2}}, \qquad (6)$$

the expressions further illustrate that the size of beam radius influences the expected spot position.

III. PROPOSED NEURAL NETWORK ENSEMBLE

This section proposes a stacking-based neural network architecture, where the final estimation is made by a meta-learner that intelligently combines the predictions of base learners.

A. Base Learner Selection

Generally, RBFNN that use a Gaussian function are good for interpolation because they make a local approximation to nonlinear input-output mapping. Furthermore, RBFNN do not have a problem with local minima, which allows for better generalization. Therefore, we have constructed all level zero learners using RBFNN.
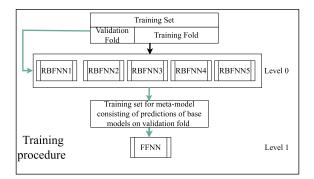
Fig. 3.   Proposed ensemble training procedure.

B. Meta Learner Selection

FFNN are better suited for extrapolation as they make global approximations to nonlinear input-output mapping. To complement the interpolation capabilities of RBFNN, we have constructed the meta learner using FFNN. According to the universal approximation theorem for FFNN [14], an ANN utilizing backpropagation algorithm, having a solitary hidden layer and adequate number of neurons, can approximate an arbitrary nonlinear function regardless of its complexity. This work employs a single hidden layer architecture for the sake of simplicity.

C. Ensemble Development

Figure 3 depicts the ensemble training procedure. The ensemble has five level-0 RBFNNs and a FFNN meta learner. During inference, the five base learners operate in parallel followed by the meta-learner, hence the additional time delay is minimal to accommodate real-time operation.

Base learners take photoelectric signals as inputs. To achieve diversity among base learners, [15] suggests three approaches, we use different spread values for each base learner by varying this parameter from 0.2 to 1 with a precision of 0.2. Base learners' predictions form features for training the meta learner and they are generated through K-fold cross validation technique. Where, the training set is divided into K folds, the base learners are trained on a sample of $K-1$ folds and then make predictions on the out of sample fold. By repeating this process K times, with a unique out of sample fold each time, the meta learner training data is generated.

The meta-learner of the $5-8-1$ architecture with a logistic sigmoid transfer function is trained through backpropagation. Early stopping criteria is employed to avoid over-fitting the meta-learner by setting aside 15% of the training data for validation and terminating the training whenever the error on the validation set starts to increase. Algorithm 1 summarises the stacking ensemble procedure.

Maximum error (Max_{error}), mean absolute error (MAE), and root mean squared error (RMSE) are used to evaluate the performance of the developed model. They are defined as:

$$Max_{error} = \max\{|t_i - p_i|\}, \quad i = 1, 2, 3 \ldots N, \quad (7)$$

$$MAE = \frac{1}{N} \sum_{i=1}^{N} |t_i - p_i|, \quad (8)$$

Algorithm 1 Stacking Ensemble

Input : 1. Training data
                2. T level-0 learning algorithms
Output: Neural network ensemble

1 **Initialization:** 1. *Storage for trained base learners*
    2. *Randomly divide the training set into K folds*
2 **for** $j = 1, \ldots, T$ **do**
3   - Create a base learner
4   **for** $l = 1, \ldots, K$ **do**
5   - Train the base learner on $K-1$ folds
6   - Make predictions on the Kth out of sample fold
7   - Store the predictions
8   **end**
9   - Train the base learner on the whole training set
10   - Add the trained model to the ensemble
11 **end**
12 - Train a meta learner using the Kth fold predictions
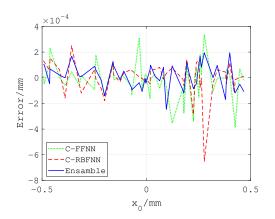

Fig. 4.   Error comparison between ensemble and the complex models by considering 0.75 mm beam radius.

$$RMSE = \sqrt{\frac{1}{N} \Sigma_{i=1}^{N} \left(t_i - p_i\right)^2}, \quad (9)$$

where N denotes the number of examples, p_i is the ith predicted value and t_i is the ith actual value.

IV. SIMULATIONS AND RESULTS

Simulations are conducted in MATLAB R2023a using experimental data from [8]. The data was collected from a QD with a 1.5 mm radius and a range of -0.5 mm to 0.5 mm along the x axis was observed on the QD. The incident beam radii were at 0.55 mm, 0.75 mm, 0.95 mm, and 1.15 mm. Sets of 501 samples from each beam radius are used and subsequently divided into 451 training and 50 testing samples. The proposed ensemble learning algorithm is compared to the FFNN in [8] and the RBNN network in [11] as well as to FFNN and RBNN employing the same number of parameters as the proposed ensemble in one hidden layer, which are named C-FFNN and C-RBFNN, respectively. With a 0.75 mm beam radius, the error performance as a function of **x**-axis is shown in Fig. 4. The ensemble model demonstrates reduced error fluctuations compared to the other two models of similar complexity.

TABLE I
PERFORMANCE OF THE MODELS WITH VARIED BEAM RADIUS

0.55 mm beam radius			
	$RMSE$	Max_{error}	MAE
$FFNN$	3.2382×10^{-4}	8.8079×10^{-4}	2.5548×10^{-4}
$RBFNN$	1.2912×10^{-4}	3.1903×10^{-4}	1.0310×10^{-4}
$C-FFNN$	1.5642×10^{-4}	4.5075×10^{-4}	1.2232×10^{-4}
$C-RBFNN$	2.2175×10^{-4}	6.7030×10^{-4}	1.2627×10^{-4}
$Ensemble$	9.0755×10^{-5}	3.0192×10^{-4}	7.0253×10^{-5}
0.75 mm beam radius			
	$RMSE$	Max_{error}	MAE
$FFNN$	1.7261×10^{-4}	4.8105×10^{-4}	1.3232×10^{-4}
$RBFNN$	1.3285×10^{-4}	3.5378×10^{-4}	1.0138×10^{-4}
$C-FFNN$	1.4717×10^{-4}	3.8675×10^{-4}	1.0167×10^{-4}
$C-RBFNN$	1.3212×10^{-4}	6.5112×10^{-4}	8.5137×10^{-5}
$Ensemble$	9.7828×10^{-5}	2.5457×10^{-4}	7.4144×10^{-5}
0.95 mm beam radius			
	$RMSE$	Max_{error}	MAE
$FFNN$	3.2839×10^{-4}	7.5519×10^{-4}	2.6410×10^{-4}
$RBFNN$	3.6206×10^{-4}	8.2480×10^{-4}	2.9773×10^{-4}
$C-FFNN$	2.5851×10^{-4}	8.8196×10^{-4}	1.9476×10^{-4}
$C-RBFNN$	2.0197×10^{-4}	9.3183×10^{-4}	1.2477×10^{-4}
$Ensemble$	1.1814×10^{-4}	3.8161×10^{-4}	9.4459×10^{-5}
1.15 mm beam radius			
	$RMSE$	Max_{error}	MAE
$FFNN$	2.2227×10^{-4}	5.1770×10^{-4}	1.7560×10^{-4}
$RBFNN$	1.2912×10^{-4}	3.1903×10^{-4}	1.0310×10^{-4}
$C-FFNN$	1.2623×10^{-4}	3.2932×10^{-4}	9.7709×10^{-5}
$C-RBFNN$	1.1121×10^{-4}	3.6490×10^{-4}	7.6820×10^{-5}
$Ensemble$	9.5239×10^{-5}	3.6948×10^{-4}	7.2360×10^{-5}

Table I presents results (in mm) for the different models in comparison. The proposed model has superior performance for all beam radii. Considering the 0.75 mm beam radius, as an example, the proposed model achieves RMSE, which is 26.36% lower than RBFNN [11] and 43.32% lower than FFNN [8]. Compared to the ANNs of the same complexity, the ensemble achieves RMSE of 33.53% lower than C-FFNN and 25.59% lower than C-RBFNN.

V. CONCLUSION

An ensemble of ANNs is proposed to improve the performance of QD. Previous studies considered single ANN models, which could be affected by the intrinsic limitations of the individual ANN,i.e. the inability to learn all underlining features. On the contrary, in an ensemble, limitations of one learner are alleviated by the other learners. The proposed solution outperforms both FFNN and RBFNN even for the same number of parameters, i.e. complexity, making it a viable choice for an improved QD position estimation.

REFERENCES

[1] E. A. Park, D. Cornwell, and D. Israel, "NASA's next generation = 100 Gbps optical communications relay," in *Proc. IEEE Aerosp. Conf.*, Mar. 2019, pp. 1–9.

[2] M. Z. Chowdhury, Md. T. Hossan, A. Islam, and Y. M. Jang, "A comparative survey of optical wireless technologies: Architectures and applications," *IEEE Access*, vol. 6, pp. 9819–9840, 2018.

[3] A. B. Raj and A. K. Majumder, "Historical perspective of free space optical communications: From the early dates to today's developments," *IET Commun.*, vol. 13, no. 16, pp. 2405–2419, Oct. 2019.

[4] J. Zhang, M. A. Itzler, H. Zbinden, and J.-W. Pan, "Advances in InGaAs/InP single-photon detector systems for quantum communication," *Light, Sci. Appl.*, vol. 4, no. 5, p. e286, May 2015.

[5] X. Wang, X. Su, G. Liu, J. Han, K. Wang, and W. Zhu, "A method for improving the detection accuracy of the spot position of the four-quadrant detector in a free space optical communication system," *Sensors*, vol. 20, no. 24, p. 7164, Dec. 2020.

[6] C. Zhang, F. Duan, X. Fu, W. Liu, Y. Su, and X. Li, "Research of intelligent segment-fitting algorithm for increasing the measurement accuracy of quadrant detector in straightness measuring system," *Opt. Laser Technol.*, vol. 125, May 2020, Art. no. 106062.

[7] E. C. C. M. Silva and K. J. V. Vliet, "Robust approach to maximize the range and accuracy of force application in atomic force microscopes with nonlinear position-sensitive detectors," *Nanotechnology*, vol. 17, no. 21, pp. 5525–5530, Nov. 2006.

[8] Q. Li, J. Wu, Y. Chen, J. Wang, S. Gao, and Z. Wu, "A new response approximation model of the quadrant detector using the optimized BP neural network," *IEEE Sensors J.*, vol. 20, no. 8, pp. 4345–4352, Apr. 2020.

[9] Z. Qiu, W. Jia, X. Ma, B. Zou, and L. Lin, "Neural-network-based method for improving measurement accuracy of four-quadrant detectors," *Appl. Opt.*, vol. 61, no. 9, p. F9, 2022.

[10] C. Lu, Y.-S. Zhai, X.-J. Wang, Y.-Y. Guo, Y.-X. Du, and G.-S. Yang, "A novel method to improve detecting sensitivity of quadrant detector," *Optik*, vol. 125, no. 14, pp. 3519–3523, Jul. 2014.

[11] X. Wang, X. Su, G. Liu, J. Han, W. Zhu, and Z. Liu, "Method to improve the detection accuracy of quadrant detector based on neural network," *IEEE Photon. Technol. Lett.*, vol. 33, no. 22, pp. 1254–1257, Nov. 15, 2021.

[12] J. Wu and E. Chen, "A novel nonparametric regression ensemble for rainfall forecasting using particle swarm optimization technique coupled with artificial neural network," in *Proc. 6th Int. Sym. Neural Netw.* Cham, Switzerland: Springer, 2009, pp. 49–58.

[13] H. Kaushal et al., "Acquisition, tracking, and pointing," in *Free Space Optical Communication*. New Delhi, India: Springer, 2017, pp. 119–137.

[14] G. Cybenko, "Approximations by superpositions of a sigmoidal function," *Math. Control, Signals Syst.*, vol. 2, pp. 183–192, Jan. 1989.

[15] D. Wang and Y. Li, "A novel nonlinear RBF neural network ensemble model for financial time series forecasting," in *Proc. 3rd Int. Workshop Adv. Comput. Intell.*, Aug. 2010, pp. 86–90.